scientific reports

Check for updates

OPEN

Uncovering pre-cytokinetic block in cancer cells under shear stress using a disturbed flow-generating device

Lucie Beresova[1], Jan Vitecek[2,7,8], Iva Protivánková[1], Michal Dudka[5], Katarina Chroma[1], Zdenek Skrott[1], Tereza Buchtova[3], Kamila Poláková[2], Jan Novotny[6], Ludmila Novakova[6], Jiri Bartek[1,3,4] & Martin Mistrik[1]✉

During metastasis, cancer cells navigate through harsh conditions, including various mechanical forces in the bloodstream, highlighting the need to understand the impact of mechanical and shear stresses on cancer cells. To overcome the current methodological limitations of such research, here we present a new device that replicates similar conditions by applying shear stress on cultured cells. The device provides a less complex, easily accessible alternative to traditional fluidics while generating fluid shear stress values comparable to those in human veins and capillaries. The device allows analyses of large cell numbers in standard cell culture flasks and incubators. Using this device to explore the shear stress-induced responses of various human cell lines, we discovered a previously unknown, reversible pre-cytokinetic block occurring in cells that lose anchorage during mitosis and are kept under constant shear stress. Notably, some cancer cell lines appear to bypass this unorthodox cell-cycle block, suggesting its role as a safety checkpoint to restrict the proliferation of cancer cells in the bloodstream and their overall spreading potential. These findings provide new insights into the diverse responses of normal and cancer cells to shear stress and highlight the potential of our technology for research on circulating tumor cells and metastatic spread.

Keywords Fluid shear stress, Circulating tumor cells, Fluidic systems, Metastasis, Mitosis

Cancer metastasis, an often incurable, terminal disease stage, is responsible for approximately 90% of cancer-related deaths[1]. Cancer cells are subjected to numerous factors and stressors throughout their journey from primary tumors to distal tissues, including specific physical forces. Fluid shear stress, experienced within the blood and lymphoid vessels and interstitial fluid, significantly impacts circulating cancer cells[2,3]. Despite its acknowledged importance, the effect of shear stress on cancer cells, and more broadly on human cells, is not well understood[4]. This gap in our knowledge is primarily due to currently limited technological possibilities. Aside from sophisticated single-cell analysis methods applied to cells isolated from a patient's peripheral blood circulation[5,6], most studies addressing shear stress rely on fluidic systems that closely simulate fluid circulation in vessels. However, these systems typically aren't compatible with suspension cells, limiting their application to adherent cells only[2,7]. A further constraint of fluidics is the limited number of cells that can be examined at any given time. This results in a limited understanding of the biology of circulating cells, including circulating tumor cells (CTCs).

Our present study aims to fill this crucial knowledge gap by designing, constructing, validating, and applying a novel device—the shear stress generator (SSG), an experimental tool capable of mimicking the physiological

[1]Laboratory of Genome Integrity, Faculty of Medicine and Dentistry, Institute of Molecular and Translational Medicine, Palacky University, Olomouc, Czech Republic. [2]Department of Biophysics of Immune System, Institute of Biophysics of the Czech Academy of Sciences, Kralovopolska 135, Brno, Czech Republic. [3]Danish Cancer Institute, Danish Cancer Society, Copenhagen, Denmark. [4]Division of Genome Biology, Department of Medical Biochemistry and Biophysics, Science for Life Laboratory, Karolinska Institute, Stockholm, Sweden. [5]Department of Optics, Faculty of Science, Palacky University, Olomouc, Czech Republic. [6]Faculty of Mechanical Engineering, Jan Evangelista Purkyně University, Ústí Nad Labem, Czech Republic. [7]International Clinical Research Center, St. Anne's University Hospital Brno, Brno, Czech Republic. [8]Department of Biochemistry, Faculty of Medicine, Masaryk University, Kamenice 5, Brno 625 00, Czech Republic. ✉email: martin.mistrik@upol.cz

fluid shear stress conditions the cells experience in blood vessels. We document here that this technology provides new insights into how shear stress impacts the behavior of cancer cells, thereby paving the way for a better understanding of cancer metastasis and contributing to developing more effective anticancer treatment strategies. Leveraging this versatile approach, here we have examined the impact of shear stress on significantly larger numbers of cells and discovered a previously unknown biological phenomenon critical for the fate of the mitotic cells that are transiting into a suspension mode.

Results

Construction and characterization of the shear stress generator (SSG)

The device is composed of a clip-like platform that holds a standardized 150 cm^2 cell culture flask connected to the rotor of a stepper motor (Fig. 1a,b). A custom-made program drives the stepper motor to oscillate the flask in a horizontal plane. This movement acceleration triggers a recurring wave of media within the flask.

The flow speed's primary component aligns with the flask's direction. However, near the flask's neck, a perpendicular component to this motion deviates the overall trend from perfect linearity. Upon hitting the flask's sidewalls, the wave also generates slight turbulence accompanied by bubble formation.

To better understand the flow conditions within the moving flask, we developed a computational fluid dynamics (CFD) model to simulate the free surface flow. The CFD visualization of the standard setup (used for most biological experiments) involving dangling ± 47.5° within a 2.44 s period revealed that the recurring wave propagating across the flask is accompanied by a wave of elevated shear stress (Fig. 2a and Supplementary video 1).

In total, we analyzed four different dangling periods (4.84, 2.44, 1.57, and 1.22 s), all with the same oscillation angle of ± 47.5°, over several cycles. As shown in the chart and summary table (Fig. 2b,c), the 4.84 s, 2,44 s, and 1.57 s regimes exhibit increasingly pronounced weighted average shear stress across the flask bottom as the period decreases. These changes are driven by stronger interactions between the liquid and the vessel walls, as the fluid experiences higher acceleration and deceleration during oscillation. In the regime with a 2.44-s period, some asymmetry may occur, which could be attributed to the dynamics of the return wave reflected from the vessel wall.

Interestingly, in the regime with a 1.22-s period (the fastest dangling), simulations indicate that the liquid already reaches the vessel's lid, resulting in a more uniform shear stress distribution across the bottom. This is reflected in the time course of shear stress, which is relatively consistent and lower than the slower regimes. The sudden decrease in the shear stress values may be due to the vertical movement of the fluid reducing the influence of wall interactions on shear stress at the bottom. The effect of the liquid reaching the vessel's lid was indeed confirmed experimentally, as shown in the accompanying images (Supplementary Fig. 2a).

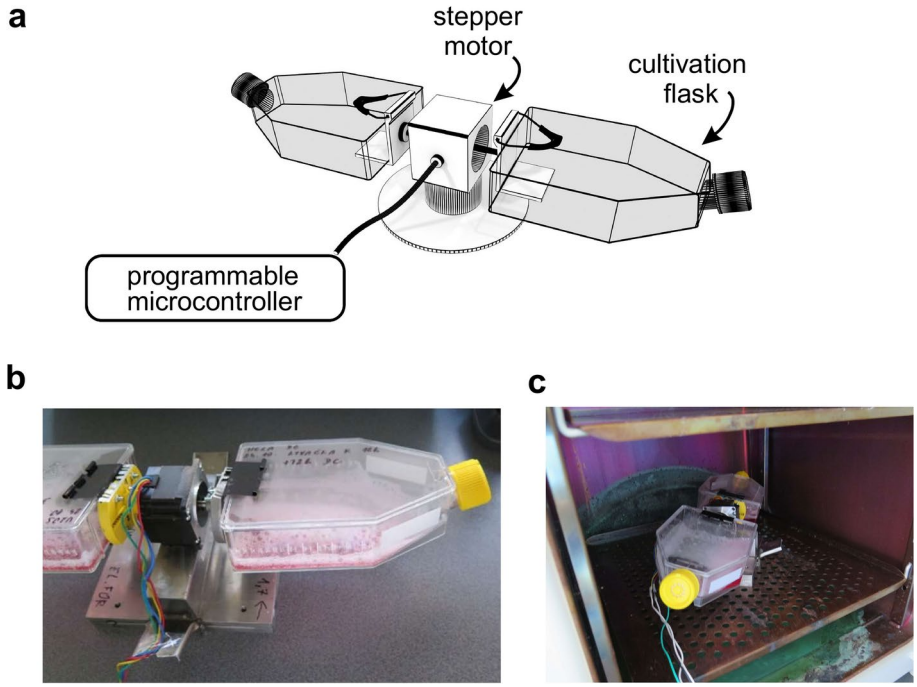

Fig. 1. Design of the shear stress generator. (**a**) Schematic representation of the shear stress generator involving the stepper motor, two clips holding the standardized 150 cm^2 cell cultivation flasks, and stepper motor controller. The flask's axis aligns with the stepper motor's axis; hence, the bottom of the flask is located 21.5 mm below the rotation axis. (**b**) Photograph of the actual device used for the study (**c**) Placement of the device inside a standard CO_2 cell culture incubator.

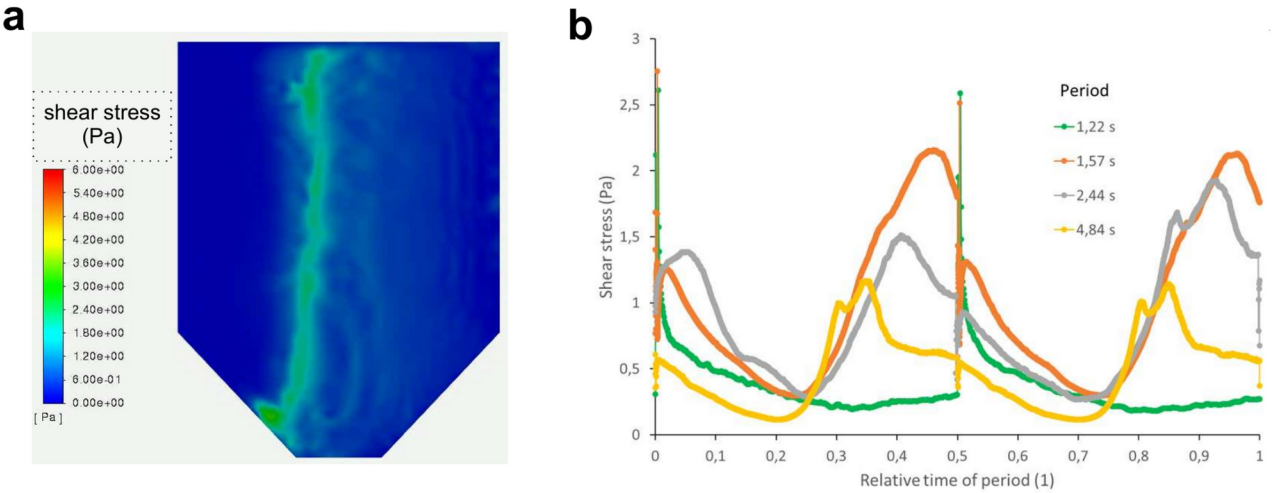

c

Period (s)	Weighted average shear stress (Pa)			
	Mean	SD	Min	Max
4.84	0.49	0.30	0.11	1.17
2.44	0.90	0.48	0.27	1.93
1.57	1.31	0.61	0.30	2.75
1.22	0.36	0.23	0.18	2.61

Fig. 2. Quantification of generated fluid shear stress. (**a**) Image from computational fluid dynamics (CFD) simulation of the free surface flow depicting actual shear stress at a particular position and time for standard setup (**b**) Comparison of weighted average shear stress across the flask bottom induced by various dangling regimes in a standardized 150 cm^2 flask with a ± 47.5° oscillation angle and periods of 4.84, 2.44, 1.57, and 1.22 s, respectively. For clarity, time is expressed relative to the period (1 = one complete period), with the starting point at maximum flask rotation. (**c**) Comparison of weighted average shear stress across the flask bottom induced by dangling regimes in a 150 cm^2 flask with a ± 47.5° oscillation angle and periods of 4.84, 2.44, 1.57, and 1.22 s, respectively.

Calculated values for the standard 2.44-s period revealed the weighted average shear stress reaching values 2.7–19.3 dyne/cm^2, with a mean value of 9.0 dyne/cm^2 (corresponding to 0.27—1.93 Pa and 0.9 Pa, respectively). Importantly, these values align with the levels reported for the human venous system[8–10] (Fig. 2b,c).

An essential feature of the experimental setup is its long-term stability. The device is capable of continuous operation for several days without any failures or undesirable changes in the movement and, thus, shear stress values. The system also requires a relatively low amount of energy—approximately 7W for two standardized 150 cm^2 flasks—making it suitable for use in cell incubators, which are not commonly equipped with active cooling and thus limit the placement of high-power devices.

Biological relevance and impact of generated shear stress

Following the mathematical characterization of the device, we next investigated the occurrence of some typical shear stress-induced phenotypes on cultured mammalian cells. Initially, we evaluated the elongation of endothelial cells (ECs) according to the flow vector[11]. This physiological response naturally occurs in the vasculature and can be simulated in fluidic systems using a specialized cultivation chamber, pumps, and valves to ensure a defined media flow[8]. Indeed, the media flow under our standardized SSG experimental conditions was sufficient to trigger this typical cellular elongation process comparable with a commercial fluidics system by IBIDI (Fig. 3a,b).

In order to see if cells are perceiving shear stress at the molecular level, we examined selected ECs' mechanosensory and signaling pathways. Several pathways have been established in flow sensing by EC[12]. These mechanosensitive pathways become activated within seconds to hours and may return to baseline state within 24 h of exposure to flow[13–18]. Since the dangling rather induces oscillatory flow, we determined the expression of disturbed fluid flow markers in EC: ICAM-1 and VCAM-1[15,19]. It was carried out at two typical time points reflecting expression changes (48 h) and adaptation of the cells to the flow (72 h). Whereas the ICAM-1 transcript showed a transient increase at 48 h, returning to normal levels at 72 h, the VCAM-1 transcript stayed permanently elevated (Fig. 4a). Such data can be interpreted to mean cells indeed perceived the flow to which they adapted (ICAM-1)[15]; however, the flow has rather disturbed as demonstrated by persistently elevated VCAM[19] over 72 h. Notably, for setting with doubled dangling time (oscillation period of 4.84 s leading to lower shear stress values), the onset of ICAM-1 is delayed (not significant before 72 h), while VCAM-1 does not

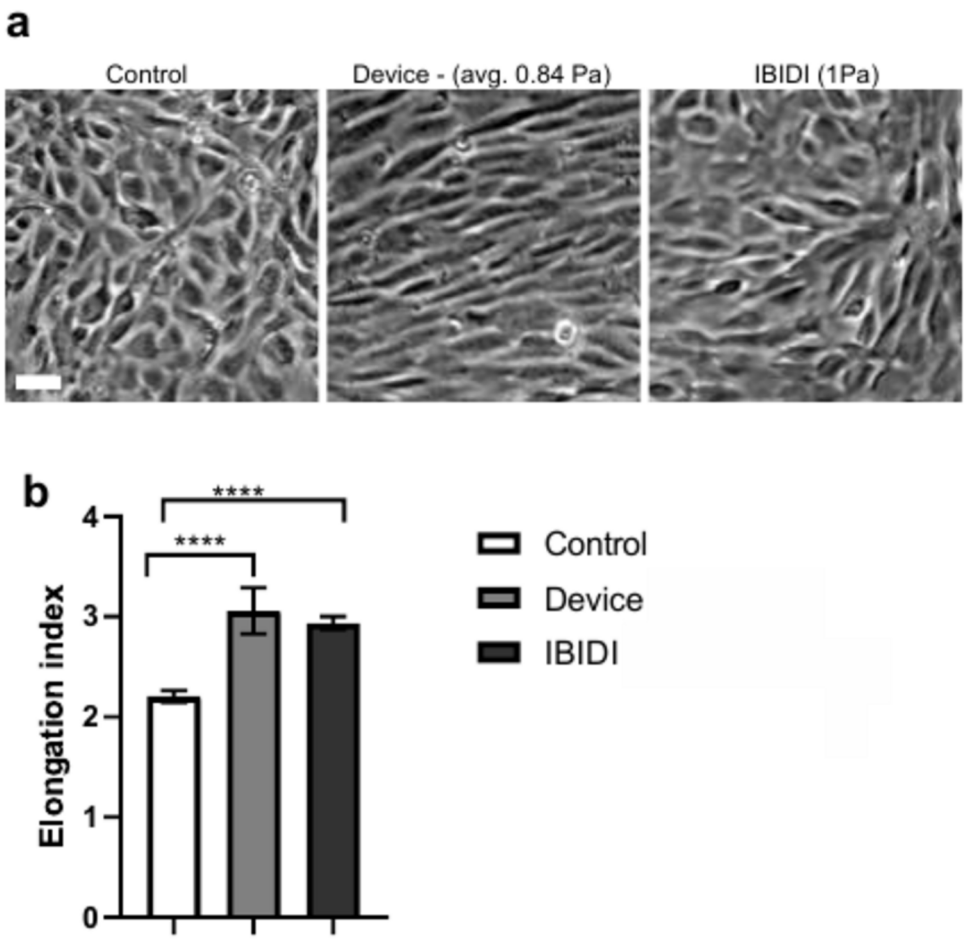

Fig. 3. The medium flow effect on elongation of the MS1 murine endothelium cells: Cells were subjected to standard cultivation conditions, fluid shear stress induced by the shear stress generator at standard setup (mean value 0.9 Pa), and compared to fluid shear stress induced by commercial fluidics system by IBIDI (1 Pa) for 5 days. (**a**) images depicting the alignment and elongation of cells. (**b**) The quantitative comparison of the elongation indexes (ratio of the major to the minor axis of an ellipse circumscribed to cells). The elongation index was determined by image analysis. Data are given as mean ± SD. Each data point represents descriptors of at least 9000 cells in two biological replicates, each having at least three technical replicates. An unpaired two-tailed t-test was used for *p*-value calculation, with statistical significance ****$p < 0.0001$. Microscopic images show the typical shape of cells after 48 h of treatment. The bar indicates 50 µm.

respond within 72 h (Supplementary Fig. 1a). Additionally we compared the response of these two markers with the commercial fluidics system by IBIDI after 24 h in a setup roughly mimicking shear stress forces induced by the device (oscillatory flow, 2 s period and shear stress 1 Pa). Interestingly, the response was comparable despite the much narrower wave of the shear stress produced by the device (Supplementary Fig. 2b).

Further, the immediate shear stress perception onset was assayed through the phosphorylation status of major protein kinases involved in response to flow[16–18]. The Erk1/2 kinase showed transient phosphorylation within 5 min from flow onset. The maximum phosphorylation of Akt kinase was delayed to 30 min—2 h. Instead, the phosphorylation of JNK and P38 kinases showed a steady increase up to 6 h of the experiment duration (Fig. 4b). Interestingly, the early transient phosphorylation of ERK1/2 indicates the perception of steady flow[16], whereas the phosphorylation pattern of Akt, JNK, and P38 kinases was consistent with the general perception of flow[17,18]. Interestingly, the same responses were also observed for devices' settings with doubled dangling time (lower shear stress) (Supplementary Fig. 1b). Taken together, the cells were able to sense the shear stress generated by the device. Such shear stress was rather perceived as a blend of laminar and disturbed characteristics.

In summary, these findings suggest that the presented device is applicable in various studies assessing cellular responses to shear stress and thus provides a possible alternative or an addition to experimental strategies currently dependent on fluidic systems.

Fluid shear stress induces a pre-cytokinetic block

If exposed to the mechanical forces generated by our device, several adherently growing cell lines release cells into suspension during mitosis. This effect is due to the relatively weaker adhesion of mitotic cells to the cultivation surface, commonly referred to as mitotic shake-off [20]. Importantly, this mechanism might be highly relevant for

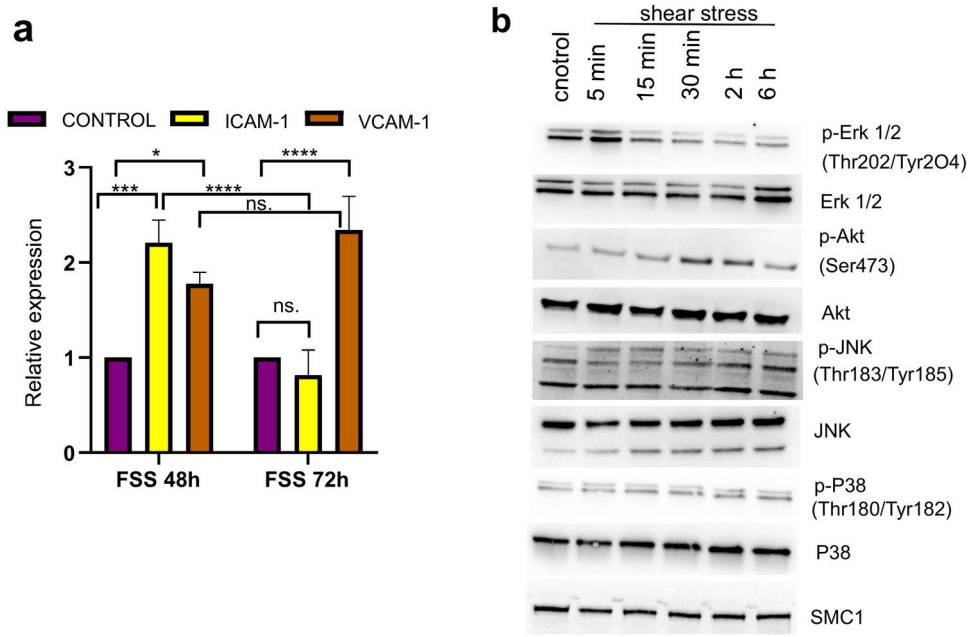

Fig. 4. Mechanosensitive response of MS1 murine endothelium cells to generated fluid shear stress. (**a**) Transcriptional response of mechanosensing markers. Control cells and cells cultivated on the shear stress generator under standard setup (mean value 0.9 Pa) for 48 h and 72 h were analyzed using qPCR. Data are given as relative values compared to the control and displayed as mean ± SD. The experiment was performed in three independent biological replicates (n = 3). An ordinary one-way ANOVA test with Sidak's multiple comparison test was used for *p*-value calculation. Relevant comparisons are shown (ns, not significant; $*p < 0.05$; $***p < 0.001$) $****p < 0.0001$). (**b**) Western blot analysis of posttranslationally activated (phosphorylated) mechanosensing markers after exposure of MS1 cells to the fluid shears stress under standard setup (mean value 0.9 Pa) at different time points. SMC1 protein was used as a loading control.

potential tumor cell dissemination. At least some circulating tumor cells (CTCs) may originate from mitotic cells dislodged from the primary tumor just by the mechanical forces caused by blood or plasma flow.

Taking advantage of our device's compatibility with cells in suspension and long-term applications, we followed the fate of the released mitotic cells under continuous fluid shear stress conditions. In human primary fibroblast strain BJ, as well as some cancer cell lines such as U-2-OS osteosarcoma, MDA-MB-231, MCF7 and BT549 breast cancers, and A549 lung cancer, the released mitotic cells were unable to complete the final phase of cytokinesis which under normal circumstances leads to daughter cells separation. The resulting binucleate-like cells were subjected to microscopic analysis, revealing incomplete cleavage with a persisting actin-myosin contractile ring (Fig. 5a,b).

Next, we tested the ability of these bi-nucleated cells to survive under conditions mimicking those that cells likely experience in the bloodstream, i.e. under continuous shear stress cultivation over prolonged periods. For this experiment, we collected the bi-nucleated cells after 18 h of cultivation under shear stress conditions. Cells were counted, placed into a new cultivation flask, and cultivated for another 24 and 48 h. The number of cells was then compared to that at the starting point of this long-term experiment. In all models tested, the prolonged cultivation of bi-nucleated cells under continuous shear stress turned to be highly cytotoxic (Fig. 6a), suggesting an important role of this newly identified cell cycle pre-cytokinetic block in regulating cell survival under shear stress and thereby possibly limiting the potential of cancerous cells for metastatic spread.

Interestingly, and in contrast to the cell models mentioned above, some of the other human cancer cell lines that we tested, including SiHA and HeLa S3 (established from a cervical carcinoma), PC3 (prostate cancer), and Cal51 (breast cancer), showed a different behavioral pattern. Thus, while the latter cancer models also accumulated cells in suspension under continuous shear stress conditions, the occurrence of binucleated cells with incomplete cytokinesis within the suspension fraction, as described above, was sporadic, reflecting a relatively normal mitotic process resulting into timely and complete daughter cell separation. After exposing such cellular suspensions to continuous shear stress over prolonged periods, we found a cytostatic rather than cytotoxic effects for SiHA, PC3, and Cal51 cell lines and surprisingly normal ongoing proliferation for HeLa S3 cells (Fig. 6b).

In conclusion, our findings presented in this section show that most human cell lines of our panel subjected to continuous shear stress release mitotic cells, and furthermore, the shear stress triggers mechanisms that interrupt the cell cycle just before cytokinesis. At the same time, the released cells are incapable of long-term survival in such a state. On the other hand, some cancer cells can bypass this safety mechanism, which might have significant consequences for tumor dissemination potential.

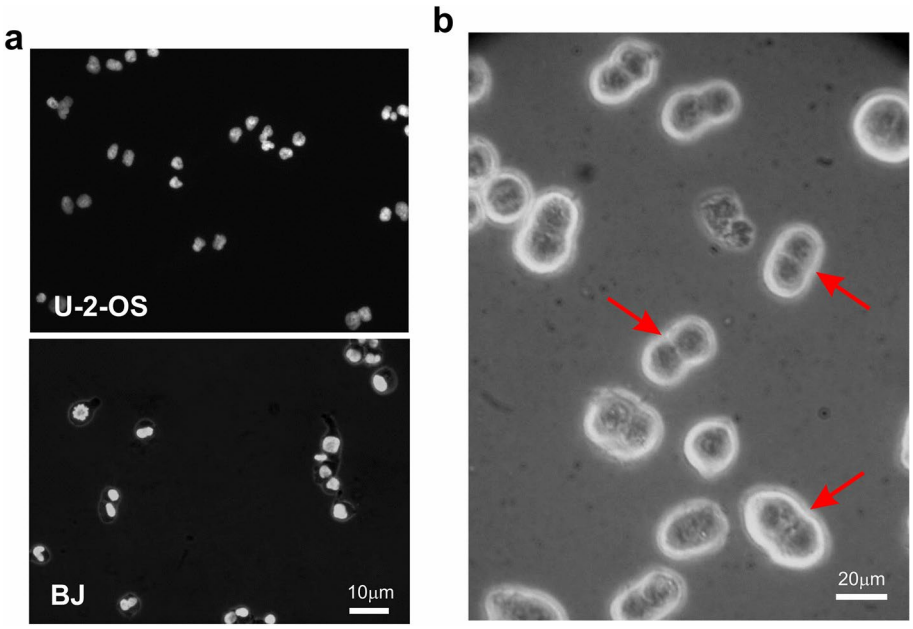

Fig. 5. Interrupted cytokinesis in mitotic cells under fluid shear stress conditions. (**a**) Fluorescence images depicting suspension of binuclear-like cells accumulating under continuous fluid shear stress conditions. Cells were cultivated on the shear stress generator generating fluid shear stress (mean value 0.9 Pa) for 18 h; the suspension fraction was stained by HOECHST DNA stain and evaluated under a fluorescent microscope (upper image U-2-OS cells, lower image BJ primary fibroblasts). The population also contains mononuclear cells representing freshly released mitotic cells (recognizable by condensed chromosomes). (**b**) Detail of the binuclear-like cells (U-2-OS) using phase contrasted transmission light microscopy with visible actin-myosin contractile rings (marked by arrows).

Reversibility of the pre-cytokinesis cell cycle block

As nothing is known about this pre-cytokinesis cell cycle block induced by shear stress, we next examined its reversibility. We used U-2-OS cells as a model cell line and cultivated them on the shear stress device for 18 h. The suspension fraction of cellular doublets was collected and immediately seeded. The re-seeded cells reattached and completed the cell separation process (cytokinesis). Subsequently, such divided cells entered the S phase and resumed relatively synchronized cell growth, as evidenced by the flow cytometry analysis of the DNA content at different time points (Fig. 7a). We also performed a colony formation assay (CFA) on these cells, including cells exposed to the shear stress for 18, 24, and 48 h. For the CFA, the exact amounts of live cells were seeded and compared with the control (U-2-OS cells grown under standard conditions and trypsinized just before seeding for CFA analysis). Compared to the control, the amount of colonies originating from cellular doublets was slightly reduced in the case of 18 h, and the ability to give rise to colonies decreased for the more extended cultivation periods (Fig. 7b,c).

In conclusion, we found that under continuous shear stress, the released mitotic cells were blocked just before cytokinesis, and this block is reversible in early time points.

Discussion

We believe our present study provides a significant advancement in understanding the effects of shear stress on various cell types, both normal and cancerous. Our newly designed and applied shear stress generator provides a cell culture tool that conveniently replicates some physiological conditions cells experience in the bloodstream. The technique's simplicity, cost-effectiveness, and compatibility with standard laboratory equipment and long-term operation opens new possibilities in cancer research, particularly in elucidating the often life-threatening process of tumor cell dissemination via the bloodstream.

For example, little is known about the fate of circulating tumor cells (CTCs) in the venous system, particularly in the context of their survival mechanisms and seeding potential under the mechanical stress they inevitably experience. In-vitro studies on CTCs have traditionally employed highly sophisticated fluidic systems to simulate fluid shear. However, such approaches are often limited by sample size, as the cultivation area of commonly available fluidic chambers is relatively small, and the complexity of these systems can lead to loss or damage of suspension cellular fraction. Our shear stress generator addresses most of these issues while effectively imitating the shear stress environment inside human veins. Notably, our SSG can be applied to large cell quantities, providing a cultivation surface that is two orders of magnitude larger than conventional fluidic chambers. This innovation facilitates applications in laboratory techniques that require large numbers of cells, such as western blot analysis. Additionally, our device is designed so that cells released into the suspension during the shear stress treatment are not lost or damaged within the tubing and valves, a typical issue prevalent in fluidic systems.

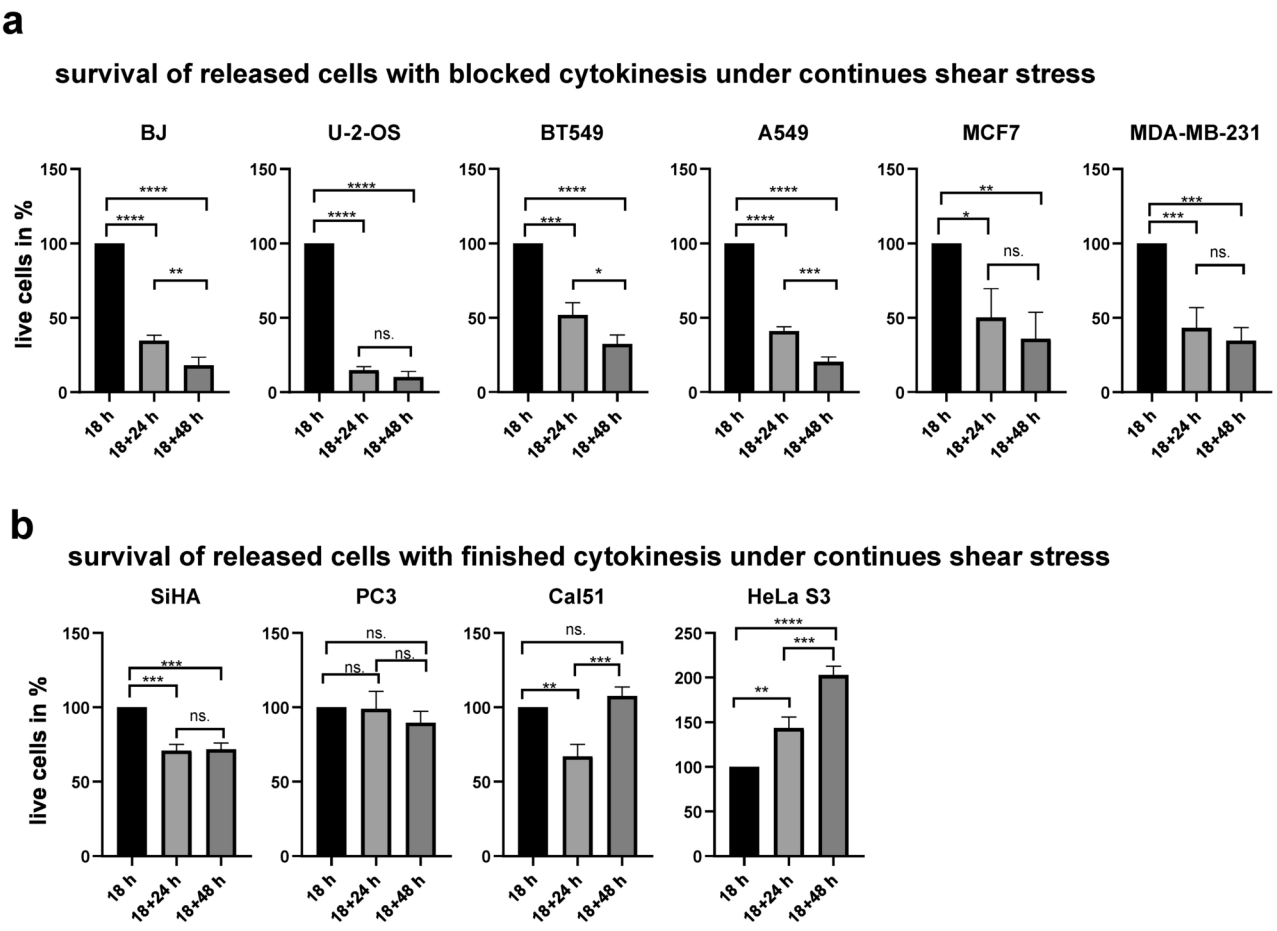

Fig. 6. Survival of released suspension cells in different cell lines under continuous shear stress conditions. Selected cell lines were cultivated on the shear stress generator generating fluid shear stress under a standard setup (mean value 0.9 Pa) for 18 h. Cell suspension fraction was collected and placed in a new flask cultivated on the shear stress generator under a standard setup (mean value 0.9 Pa) for another 24 or 48 h. (**a**) Cell lines that respond to the shear stress by accumulating cells with unfinished cytokinesis in suspension. (**b**) Cell lines that respond to the shear stress by accumulating cells with finished mitosis (binuclear-like cells are absent). All experiments were performed in three independent biological replicates (n = 3). An ordinary one-way ANOVA test with Turkey's multiple comparison test was used for *p*-value calculation. Relevant comparisons are shown (ns, not significant; $*p < 0.05$; $***p < 0.001$) $****p < 0.0001$).

The presented solution's simplicity also has limitations, primarily the inability to simulate complex conditions, such as precisely defined blood flow and pressure changes. Despite these limitations, our device can produce fluid shear stress, corresponding to values observed within the venous and possibly arterial system[8–10]. As such, our method effectively generates some of the expected shear stress-induced cellular responses, proving its potential in cellular stress research and complementing fluidics-based experiments. The shear stress generated by the device was rather a blend of laminar and disturbed characteristics, as indicated by endothelial cell response.

A pivotal finding of our study is the discovery of a cellular phenomenon related to the final stages of the mitotic process: a reversible pre-cytokinetic block observed in cells that lose anchorage during mitosis and continue to experience fluid shear stress. We propose that this block serves as a safety checkpoint, preventing cells from their potentially hazardous proliferation within the blood or lymphatic system.

Our discovery of this reversible pre-cytokinetic block adds a new dimension to the current understanding of cellular response to mechanical stress. Our data suggest the existence of cell survival mechanisms activated under harsh, shear-stress conditions, highlighting the potential relevance for cancer metastasis. Another noteworthy finding that we present was the apparent bypass of this safety cell-cycle block in some cancer cell lines. These observations raise a plethora of new questions regarding the regulation of this process and the potential genetic and epigenetic factors that allow the latter subset of cancer cells to bypass this block and its consequences for the survival and overall fate of circulating cancer cells. Of relevance, it was observed that binucleated tetraploid cells induced chemically displayed higher degrees of genomic instability and tumorigenic potential[21].

In conclusion, our newly constructed SSG device and its application in mimicking some of the physical forces inside the venous system might pave the way for more comprehensive studies on the impact of shear stress on cells. This could lead to significant progress in cancer biology, particularly in understanding cancer cell survival under specific stress conditions and during metastasis. Moreover, while our study sheds new light on the effect

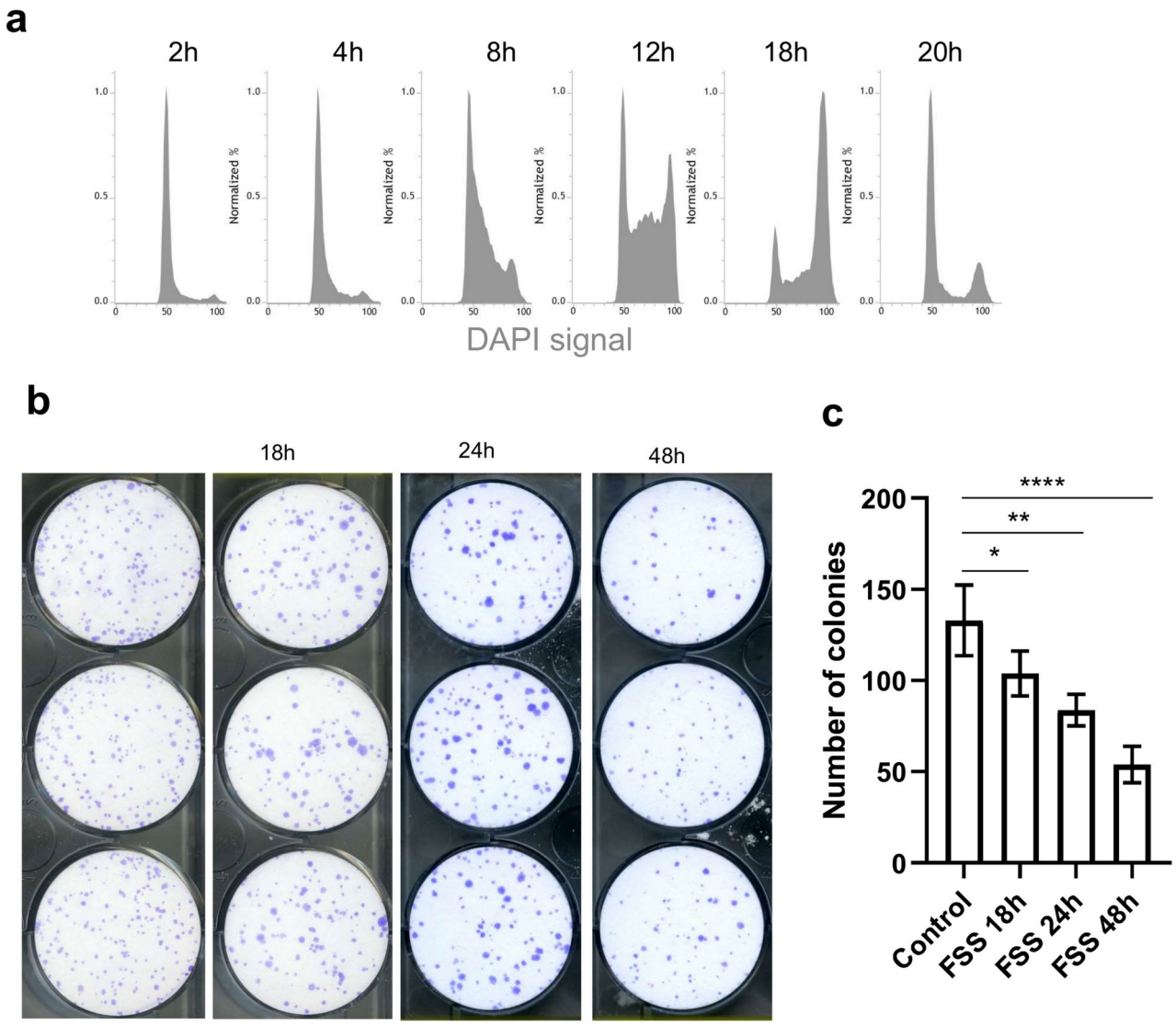

Fig. 7. Reversibility of the cytokinesis block analyzed via colony formation assay. (**a**) U-2-OS cells were cultivated on the shear stress device generating fluid shear stress under a standard setup (mean value 0.9 Pa) for 18 h. Cell suspension fraction was collected and immediately seeded for fluorescence cytometry-based cell cycle analysis. Cells were collected, fixed, and analyzed for DNA content by DAPI stain at indicated time points. (**b**, **c**) U-2-OS cells were cultivated on the shear stress device generating fluid shear stress under a standard setup (mean value 0.9 Pa) for 18 h. The suspension fraction of cells was collected and either immediately seeded for colony formation assay or placed in a new flask, which was further cultivated on the shear stress generator under a standard setup (mean value 0.9 Pa) for another 24 or 48 h, after which it was seeded for colony formation assay. Three hundred live cells were seeded into each well and compared with the control-typsinized U-2-OS cells grown under standard cultivation conditions. (**b**) Example of scored colonies for different time points. (**c**) Colony formation assay quantification.

of shear stress on the cell cycle and cellular function, the mechanism behind the observed pre-cytokinetic block and how some tumor cells can bypass this blockade remains to be elucidated. Future research in this area is needed to explore these exciting directions.

Material and methods

Details of experimental device construction

The device is composed of a clip-like platform that holds a standardized 150 cm^2 cell culture flask (TPP Cell Culture Flasks, Item No. 90150) connected to the rotor of a stepper motor (LDO-57STH41-2804B, LDO Motors). The motor is fixed to a robust stainless steel platform, ensuring stability. The center of rotation is in the middle of the flask, meaning the flask's bottom is 21.5 mm below the rotation axis. The motor is driven by the stepper motor driver board (TB6560 3A, Welleman) in the configuration: running current 2A, stop current 50%, 16 micro steps, Decay 0%, powered by 12V DC. The driver is operated by an Atmega16 (Microchip Technology)

microcontroller unit with a custom-made program (the code is available upon request) driving the motor to oscillate the flask in a horizontal plane in both directions, allowing the exact setting of the number of rotor steps and the number of steps per time unit. Our standard setup (used for most biological experiments) was set to reach rotor oscillations (i.e., flask movement) of ± 47.5° within a 2.44s period. Other periods (4.84, 1.57, and 1.22 s) were also tested, all with the fixed ± 47.5° angle.

Cell cultures

All used cell lines were obtained from ATCC, and mycoplasma was regularly tested. The list of cell lines included mice endothelial cells MS1, human breast cancer-derived MDA-MB-231, Cal51, MCF7, and BT549 cell lines, human osteosarcoma-derived U-2-OS cell line, human cervical cancer-derived SiHa and HeLa S3 cell lines, human prostate cancer-derived PC3 cell line, human lung cancer-derived A549 cell line, and human primary foreskin fibroblasts BJ. All cell lines were cultivated in DMEM (Lonza) supplemented with 10% fetal bovine serum (Thermo Fisher Scientific) and 1% penicillin/streptomycin (Sigma-Aldrich). Fetal serum for MS1 cell line cultivation was thermally inactivated (56 °C, 30 min.) before addition to media.

Determination of cellular elongation index

The determination of cell elongation was carried out using image analysis[22]. Cells in microphotographs in the transmitted light mode of observation were localized by the "Analyze Particles" function in ImageJ[23]. An ellipse was circumscribed to each cell. The elongation index was calculated as the ratio of the major to the minor axis of such an ellipse.

Experimental workflow for the shear stress generator usage

All tested cell lines were seeded on a standardized 150 cm^2 cultivation flask (TPP Cell Culture Flasks, Item No. 90150) filled with 30 ml of DMEM + 10% FBS media for 24 h before applying continuous fluid shear stress. Seeding numbers were optimized to reach approximately 80% confluency at the beginning of the experiment. The cultivation flask was located on the clip-like platform horizontally, and the device was placed in a standard cell culture CO_2 incubator. Cultivation parameters were 37 °C, 5% CO_2, and 100% humidity. For the standard setup, the device controller was set to reach rotor oscillations (i.e., flask movement) of ± 47.5° within a 2.44s period, corresponding to calculated weighted average shear stress the weighted average shear stress reaching values 2.7–19.3 dyne/cm^2, with a mean value of 9.0 dyne/cm^2 (corresponding to 0.27—1.93 Pa and 0.9 Pa, respectively). Depending on the experiment, the cells were exposed to fluid shear stress conditions for 5 min, 30 min, 18 h, 24 h, 48 h, or 72 h. Adherent cellular fractions for analysis of MS1 cells were harvested by trypsinization.

Fluidics

A fluidic chip µ-Slide I Luer (cat. No. 80176, IBIDI Gräfelfing, Germany) connected to the IBIDI pump system (cat. No. 10902, IBIDI Gräfelfing, Germany). 150 µl of suspension of MS1 cells at 1.2×10^6 to 2.5×10^6 cells per ml were loaded into a chip, and the cells were left to adhere for 2 h. The chip was connected to the fluidic unit with a total of 12 ml of culture medium to recirculate through the chip unidirectionally. Initial perfusion was set to achieve shear stress of 2 dyne/cm^2 (0.2 Pa). The shear stress was gradually incremented in 2-h intervals to reach 5, 7, and finally, 10 dyne/cm^2 (0.5, 0.7, and 1 Pa, respectively), under which the cells were kept for 5 days under a 5% CO_2 atmosphere. Medium exchange in reservoirs was carried out at 2-day intervals. For the oscillatory flow experiment, cells were prepared as above. The setup for the oscillatory flow was set according to the instruction of the IBIDI pump system operation (https://ibidi.com/30-pump-system) while keeping the shear stress 1 Pa and the period 2 s.

Computational fluid dynamics (CFD) model

In this study, we developed a CFD model to simulate the free surface flow within a standard 150 cm^2 cell culture flask attached to the oscillation device, as indicated in Fig. 1. The aim was to predict the shear stress distribution at the bottom of the vessel, which oscillated side-to-side using a stepper motor. The simulations were performed using ANSYS Fluent, a commercial CFD software. The volume of fluid (VOF) method was employed to track the free surface, and the initial conditions represented the vessel filled to the experimental level (30 ml of culture medium at 37 °C). The boundary conditions included setting the vessel walls as no-slip boundaries and modeling the top boundary as a pressure outlet with atmospheric conditions. The vessel was subjected to oscillatory motion around the y-axis, incorporating the actual angular velocity and stop time at each reversal point (using the moving frame approach). The PISO algorithm was used for pressure–velocity coupling, with the Geo-Reconstruct scheme for the VOF model. We analyzed the wall shear stress on the bottom surface over time, evaluating its mean, maximum, and minimum values during one oscillation cycle. The initial and boundary conditions ensured accurate replication of the laboratory experimental setup, and the computational setup allowed for precise simulation of the dynamic fluid behavior within the vessel.

Quantitative polymerase chain reaction (qPCR)

Total mRNA was extracted using the Qiagen extraction kit according to the manufacturer's instructions, and the extraction yield was quantified by Nanodrop (Implen). Reverse transcription to obtain cDNA was performed according to the protocol previously described[24]. qPCR was performed on LightCycler 480 Instrument II (Roche). Master mix for qPCR (total volume 12,5 µl) was prepared according to the recommended protocol for Platinum Taq DNA Polymerase used for PCR reaction (Invitrogen, cat.no 15966005). Eva Green (Biotium) intercalation chemistry was used to detect fluorescence signals. Primers used for qPCR were custom synthesized (Eurofins): VCAM-1 fw: 5′-TCTTACCTGTGCGCTGTGAC-3′; rw: 5′-GACCTCCACCTGGGTTCTCT-3′, ICAM-1 fw: 5′-CTTCCAGCTACCATCCCAAA-3′, rw: 5′-CTTCCAGGGAGCAAAACAAC-3′, ACTB fw: 5′-GCGCAAG

TACTCTGTGTGGA-3′; rw: 5′-CCGGACTCATCGTACTCCTG -3′. Each reaction was performed twice using 1 µl of cDNA. qPCR cycling parameters were denaturation at 95 °C for 10 min., 45 cycles of amplification at 95 °C for 15 s, 60 °C for 20 s, and 72 °C for 25 s. Relative quantification of gene expression was calculated using the 2-ΔΔCp method. The graphical processing and statistical significance calculation were performed in GRAPHPAD Prism 8.0.1.

Western blot analysis

Cells exposed to fluid shear stress were lysed directly into 1 × Laemmli sample buffer. The proteins in the samples were quantified with Bradford assay (ThermoFisher Scientific) according to the manufacturer's protocol. An equal amount of proteins were separated on commercial gradient 4–15% Mini Protean TGX precast gel (BIO-RAD) and transferred onto a nitrocellulose membrane. The membrane was blocked with 5% bovine milk in Tris-buffered saline containing 0.1% Tween 20 for 30 min at room temperature. Membranes were incubated with primary antibodies overnight at 4 °C and with secondary antibodies for 1 h at room temperature. Secondary antibodies were visualized by ELC detection reagent (ThermoFisher Scientific). Primary antibodies used in this study: SMC1 (Abcam ab9262; 1:2000), p-Akt(ser403)(Cell Signaling 9271S; 1:1000), Akt (Cell Signalling 9272S; 1:1000), p-JNK (Santa Cruz sc-6254;1:250), JNK (Santa Cruz sc-7345;1:250), p44/42-MAPK (ERK1/2)(thr202/tyr204) (Cell Signaling 4370S; 1:500), p44/42-MAPK (ERK1/2)(Cell Signaling 4696S; 1:1000). Secondary antibodies used in this study: goat-anti mouse IgG-HRP (GE Healthcare; 1:1000) and goat-anti rabbit (GE Healthcare; 1:1000).

Colony formation assay (CFA

Cells released by continuous shear stress were collected and centrifuged. Only live cells were counted based on trypan blue staining (Sigma Aldrich). CFA was performed by seeding 300 cells per well of 6-well plates and cultivated under standard cultivating conditions. The cells were grown for 8 days until discreet colonies were visible in a microscope. Fixation of colonies was done with 70% ice-cold ethanol, and colonies were further stained with crystal violet (Sigma Aldrich). After washed with H_2O and air-drying, the colonies were covered with edible white powdered sugar to increase the contrast. Wells were scanned using a table scanner, and colonies were counted with custom-made software analysis. The graphical processing of obtained data and statistical significance calculation were performed in GRAPHPAD Prism 8.0.1.

Flow cytometry analysis

Cells (0,5 0.10^6) were fixed with cold 4% formaldehyde for 15 min. After fixation, the cellular suspension was resuspended in PBS + 5% FBS + 2mM EDTA with 0.5 µg/ml DAPI. Samples were analyzed using a BD FACSverse flow cytometer.

Data availability

The datasets used and/or analysed during the current study available from the corresponding author (martin.mistrik@upol.cz) on reasonable request.

Received: 9 March 2024; Accepted: 11 December 2024
Published online: 22 February 2025

References

1. Chaffer, C. L. & Weinberg, R. A. A perspective on cancer cell metastasis. *Science* **331**, 1559–1564 (2011).
2. Huang, Q. et al. Fluid shear stress and tumor metastasis. *Am. J. Cancer Res.* **8**, 763–777 (2018).
3. Follain, G. et al. Fluids and their mechanics in tumour transit: Shaping metastasis. *Nat. Rev. Cancer* **20**, 107–124 (2020).
4. Fan, R. et al. Circulatory shear flow alters the viability and proliferation of circulating colon cancer cells. *Sci. Rep.* **6**, 27073 (2016).
5. Sinkala, E. et al. Profiling protein expression in circulating tumour cells using microfluidic western blotting. *Nat. Commun.* **8**, 14622 (2017).
6. Abouleila, Y. et al. Live single cell mass spectrometry reveals cancer-specific metabolic profiles of circulating tumor cells. *Cancer Sci.* **110**, 697–706 (2019).
7. Luo, C.-W., Wu, C.-C. & Ch'ang, H.-J. Radiation sensitization of tumor cells induced by shear stress: The roles of integrins and FAK. *Biochim. Biophys. Acta* **1843**, 2129–2137 (2014).
8. Chiu, J.-J. & Chien, S. Effects of disturbed flow on vascular endothelium: Pathophysiological basis and clinical perspectives. *Physiol. Rev.* **91**, 327–387 (2011).
9. Zhou, J., Li, Y. S. & Chien, S. Shear stress-initiated signaling and its regulation of endothelial function. *Arterioscler. Thromb. Vasc. Biol.* **34**, 2191 (2014).
10. Turitto, V. T. Blood viscosity, mass transport, and thrombogenesis. *Prog. Hemost. Thromb.* **6**, 139–177 (1982).
11. Shemesh, J. et al. Flow-induced stress on adherent cells in microfluidic devices. *Lab. Chip* **15**, 4114–4127 (2015).
12. World, C. J., Garin, G. & Berk, B. Vascular shear stress and activation of inflammatory genes. *Curr. Atheroscler. Rep.* **8**, 240–244 (2006).
13. Tanaka, K., Joshi, D., Timalsina, S. & Schwartz, M. A. Early events in endothelial flow sensing. *Cytoskelet. Hoboken NJ* **78**, 217–231 (2021).
14. Hahn, C. & Schwartz, M. A. The role of cellular adaptation to mechanical forces in atherosclerosis. *Arterioscler. Thromb. Vasc. Biol.* **28**, 2101–2107 (2008).
15. Nagel, T., Resnick, N., Atkinson, W. J., Dewey, C. F. & Gimbrone, M. A. Shear stress selectively upregulates intercellular adhesion molecule-1 expression in cultured human vascular endothelial cells. *J. Clin. Invest.* **94**, 885–891 (1994).
16. Bao, X., Lu, C. & Frangos, J. A. Mechanism of temporal gradients in shear-induced ERK1/2 activation and proliferation in endothelial cells. *Am. J. Physiol. Heart Circ. Physiol.* **281**, H22-29 (2001).
17. Ishida, T., Peterson, T. E., Kovach, N. L. & Berk, B. C. MAP kinase activation by flow in endothelial cells. *Circ. Res.* **79**, 310–316 (1996).
18. Mengistu, M., Brotzman, H., Ghadiali, S. & Lowe-Krentz, L. Fluid shear stress-induced JNK activity leads to actin remodeling for cell alignment. *J. Cell. Physiol.* **226**, 110–121 (2011).

19. Thayse, K., Kindt, N., Laurent, S. & Carlier, S. VCAM-1 target in non-invasive imaging for the detection of atherosclerotic plaques. *Biology* **9**, 368 (2020).
20. Taubenberger, A. V., Baum, B. & Matthews, H. K. The mechanics of mitotic cell rounding. *Front. Cell Dev. Biol.* **8**, 687 (2020).
21. Fujiwara, T. et al. Cytokinesis failure generating tetraploids promotes tumorigenesis in p53-null cells. *Nature* **437**, 1043–1047 (2005).
22. Černík, M. et al. Luminal surface plasma treatment of closed cylindrical microchannels: A tool toward the creation of on-chip vascular endothelium. *ACS Biomater. Sci. Eng.* **9**, 2755–2763 (2023).
23. Schneider, C. A., Rasband, W. S. & Eliceiri, K. W. NIH Image to ImageJ: 25 years of image analysis. *Nat. Methods* **9**, 671–675 (2012).
24. Kudlova, N. et al. An efficient, non-invasive approach for in-vivo sampling of hair follicles: Design and applications in monitoring DNA damage and aging. *Aging* **13**, 25004–25024 (2021).

Acknowledgements

The study was supported by Large RI Project LM2023050 funded by MEYS CR, the National Institute for Cancer Research project (Program EXCELES, ID Project No. LX22NPO5102), and the Grant agency of the Czech Republic: GACR 17-25976S.

Author contributions

LB, MM, and JB conceived the study; LB and MM designed most of the cellular experiments, which were performed mainly by LB and IP; MM designed and built the shear stress generator; MD built and programmed the controller for the shear stress generator; JV performed the physical and contributed to the biological qPCR-based characterization of the shear stress generator; KC performed most of the western blot analyses; TB and ZS contributed the microscopy, flow-cytometry and cellular toxicity experiments; KP performed cell elongation experiment, JN and LN developed the CFD model, MM, LB, ZS, and JB interpreted the results and wrote the manuscript, which all authors approved.

Declarations

Competing interests

The authors declare no competing interests.

Additional information

Supplementary Information The online version contains supplementary material available at https://doi.org/10.1038/s41598-024-83058-3.

Correspondence and requests for materials should be addressed to M.M.

Reprints and permissions information is available at www.nature.com/reprints.

Publisher's note Springer Nature remains neutral with regard to jurisdictional claims in published maps and institutional affiliations.